

## Supplementary Information

### Nickel vacancies tuning to tame polysulfide for Li-S batteries

Xuanyang Li,<sup>‡a,b</sup> Jian Tan,<sup>‡a,c</sup> Zhan Fang,<sup>a,c</sup> Mingxin Ye<sup>a\*</sup> and Jianfeng Shen<sup>a\*</sup>

<sup>a</sup>Institute of Special Materials and Technology, Fudan University, Shanghai 200433, China.

<sup>b</sup>Department of Chemistry, Fudan University, Shanghai 200433, China.

<sup>c</sup>Department of Materials Science, Fudan University, Shanghai 200433, China.

<sup>‡</sup>These authors contributed equally to this work

### Experimental section

**Theoretical computations.** All density functional theory (DFT) calculations were achieved by the Cambridge serial total energy package (CASTEP) in the Materials Studios package of Accelrys Inc. with the exchange-correlation functional of generalized gradient approximation (GGA) of Perdew, Burke, and Ernzerhof (PBE) method.<sup>1,2</sup> The cutoff energy for a plane wave was set at 450 eV, with a precision energy of 10<sup>-5</sup> eV and a force criterion of 10<sup>-2</sup> eV/Å for each atom. A grid of 3 × 3 × 1 Monkhorst-Pack k-points was used for geometry optimization calculations of all structures. Each unit cell of Ni<sub>3</sub>ZnC<sub>0.7</sub> contains one carbon atom. 3 × 3 slab models were adopted to simulate surface sorption and reactions with at least 25 Å vacuum to eliminate the interaction between neighboring slabs. The number of atoms of Ni, Zn, C of Ni<sub>3</sub>ZnC<sub>0.7</sub> unit cell were 81, 27, 18 and those of NiVs-Ni<sub>3</sub>ZnC<sub>0.7</sub> were 80, 27, 18 respectively. Each slab model conations two types of layers: the bottom layer was fixed as a representative of the bulk phase, while the other layers was allowed to relax with adsorbate. To prevent the interactions between periodic slabs, a 20 Å vacuum layer is applied in the direction perpendicular to the monolayer's surface. The nudged elastic band (NEB) method implemented in CASTEP was used to simulate the Li transport barriers along the pathway between the two absorptive sites on the Ni<sub>3</sub>ZnC<sub>0.7</sub> (111) and NiVs-Ni<sub>3</sub>ZnC<sub>0.7</sub> (111) surfaces. The binding energies ( $E_b$ ) of Li<sub>2</sub>S<sub>x</sub> absorbed on Ni<sub>3</sub>ZnC<sub>0.7</sub> (111) and NiVs-Ni<sub>3</sub>ZnC<sub>0.7</sub> (111) surfaces were calculated by the following equation:

$$E_b = E_{surface} + E_{Li_2S_x} - E_{total}$$

Where  $E_{surface}$  is the energy of the Ni<sub>3</sub>ZnC<sub>0.7</sub> (111) and NiVs-Ni<sub>3</sub>ZnC<sub>0.7</sub> (111) surfaces,  $E_{Li_2S_x}$  is the energy of the geometrically optimized Li<sub>2</sub>S<sub>x</sub> molecules, and  $E_{total}$  is the total energy of Li<sub>2</sub>S<sub>x</sub> absorbed on the above-mentioned surfaces.

**Fabrication of Ni<sub>3</sub>ZnC<sub>0.7</sub> and NiVs- Ni<sub>3</sub>ZnC<sub>0.7</sub> nanoparticles.** The NiZn-MOFs were synthesized using a reported methodology.<sup>3</sup> Nickel(II) nitrate hexahydrate [Ni(NO<sub>3</sub>)<sub>2</sub>·6H<sub>2</sub>O, 1.13 g] and zinc nitrate hexahydrate [Zn(NO<sub>3</sub>)<sub>2</sub>·6H<sub>2</sub>O, 0.39 g] in molar ratio of 3:1 were added to 50 mL of dimethyl formamide (DMF) under stirring for 5 min. After that, triethylenediamine (0.29 g) was dissolved in the solution above. Then A dropwise addition of a 10 mL water solution containing 1,4-benzenedicarboxylic acid (0.91 g) was made. After another 2 hours of magnetic stirring, the liquid was transferred to an 80 mL Teflon-lined autoclave and heated to 110 °C for 48 h. This was followed by washing the green powders with ethanol and separating them with centrifugation. The powders obtained subsequently dried in a vacuum oven at 55 °C for 12 h. The Ni-Zn MOF precursor was then calcined in a quartz tube furnace under an Ar atmosphere at 550 °C for 2 h to get Ni<sub>3</sub>ZnC<sub>0.7</sub> powders. Sodium borohydride (NaBH<sub>4</sub>, 0.05 g) was added to a sodium hydroxide solution (NaOH, 0.1 M, 100 mL), followed by mixing with ethanol (3 mL) and Ni<sub>3</sub>ZnC<sub>0.7</sub> (120 mg). The NiVs-Ni<sub>3</sub>ZnC<sub>0.7</sub> were produced after stirring for 25 min.

**Fabrication of NiVs-Ni<sub>3</sub>ZnC<sub>0.7</sub> and Ni<sub>3</sub>ZnC<sub>0.7</sub> functional separators.** Ultrasonic treatment was used to disperse the NiVs-Ni<sub>3</sub>ZnC<sub>0.7</sub> nanoparticles in ethanol for almost 2 hours. NiVs-Ni<sub>3</sub>ZnC<sub>0.7</sub> nanoparticles decorated polypropylene (NiVs-Ni<sub>3</sub>ZnC<sub>0.7</sub>@PP) separators were obtained by keeping a homogenous solution to stand for an additional 2 hours before collecting the supernatant for vacuum filtering. Following one day of freeze-drying, the NiVs-Ni<sub>3</sub>ZnC<sub>0.7</sub>@PP separators were produced. Ni<sub>3</sub>ZnC<sub>0.7</sub>@PP separators are manufactured in the same way as OVs-TiO<sub>2</sub>@PP, but using Ni<sub>3</sub>ZnC<sub>0.7</sub> instead.

**Preparation of polysulfides.** For the fabrication of  $\text{Li}_2\text{S}_6$  solution, S and  $\text{Li}_2\text{S}$  powders in molar ratios of 5:1 were added to the proportional mixture of 1,3-dioxolane (DOL) and 1,2-dimethoxyethane (DME) containing lithium nitrate ( $\text{LiNO}_3$ , 1wt%). After that, the mixture was heated at  $70^\circ\text{C}$  with vigorous stirring for 48h in an argon (Ar)-filled glove box.  $\text{Li}_2\text{S}_8$  solutions were also prepared by simply increasing the molar ratios of S and  $\text{Li}_2\text{S}$  powders.

**Materials characterizations.** X-ray diffraction (XRD) characterization was performed on a Bruker D8 X-ray diffractometer with a Cu K $\alpha$  X-ray source. Scanning electron microscopy (SEM) images were recorded with a Hitachi SU8010 to inspect the morphology of nanoparticles. Transmission electron microscopy (TEM) images were obtained through a JEM 2010 microscope at 200 kV. X-ray photoelectron spectroscopy (XPS) analysis were collected using an Al K (1486.6 eV) monochromatic X-ray source.

**Electrochemical measurements.** CR2032-type coin cells were commonly assembled in an Ar-filled glove box. Symmetric cells containing  $\text{Li}_2\text{S}_6$  electrolytes with NiVs- $\text{Ni}_3\text{ZnC}_{0.7}$ ,  $\text{Ni}_3\text{ZnC}_{0.7}$  and Super P electrodes were prepared. Li-S full batteries with NiVs- $\text{Ni}_3\text{ZnC}_{0.7}$ @PP,  $\text{Ni}_3\text{ZnC}_{0.7}$ @PP, and commercial PP separators are also assembled. The solution of DOL/DME (1:1 by volume) containing LiTFSI (1M) was utilized as electrolyte. Coin cells were tested in 60  $\mu\text{L}$  electrolyte. The coin cells were put through their paces on a LAND CT2001A battery test system. The electrochemical performances of all cells were evaluated at room temperature. Before the test, all cells were kept to stand for an additional 24 hours. The galvanostatic cycling tests were carried out between 1.8 and 2.6 V at various current densities.

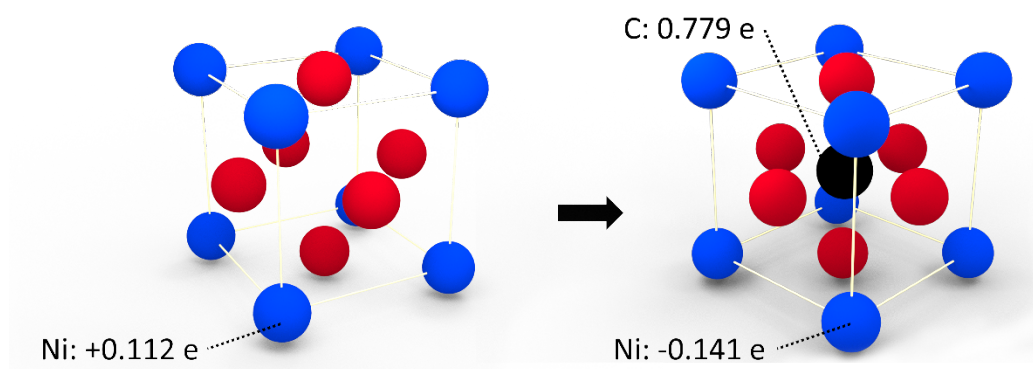


**Fig. S1.** DFT calculated optimized configurations of  $\text{Ni}_3\text{Zn}$  and  $\text{Ni}_3\text{ZnC}_{0.7}$ . In the  $\text{Ni}_3\text{Zn}$  crystal, bader charge analysis showed that each Ni atom is given  $0.112\text{ e}$  from Zn. However, In the  $\text{Ni}_3\text{ZnC}_{0.7}$  crystal, each Ni atom is given  $0.779\text{ e}$  from Zn and Ni. And nickel have an electron deficiency of  $-0.141\text{ e}$  per atom.

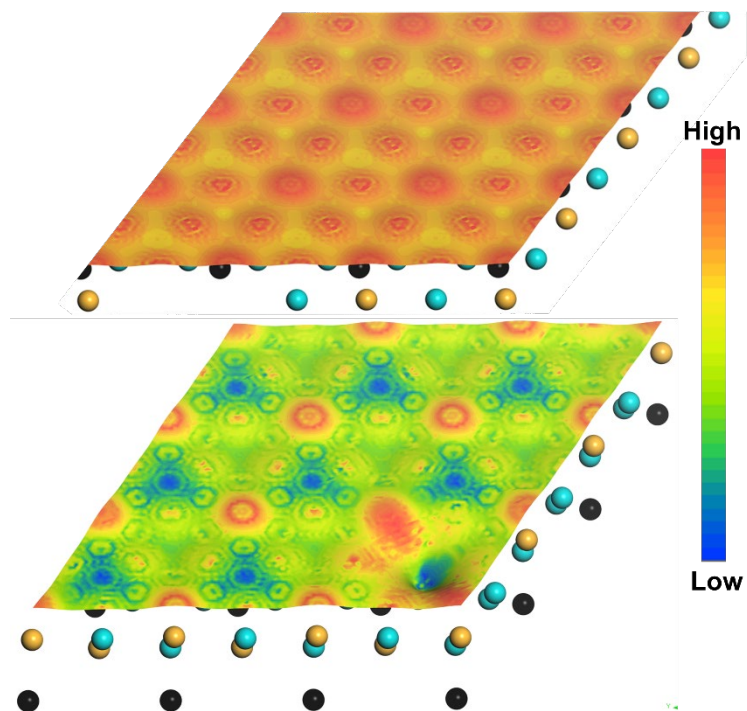


Fig. S2. DFT calculated three-dimensional isosurface ( $0.02e/\text{Bohr}^3$ ) of electron density. With the introduction of Ni vacancies, significant increase in polarity of surface is observed.

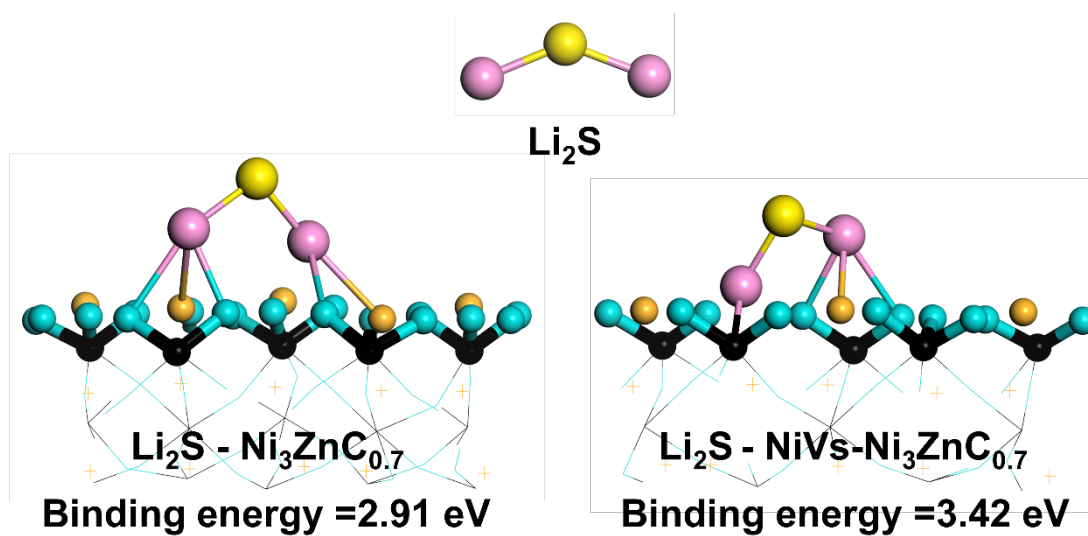


Fig. S3. DFT calculation optimized configurations of  $\text{Li}_2\text{S}$  absorbed on  $\text{Ni}_3\text{ZnC}_{0.7}$  (111) and  $\text{NiVs-Ni}_3\text{ZnC}_{0.7}$  (111) surface.

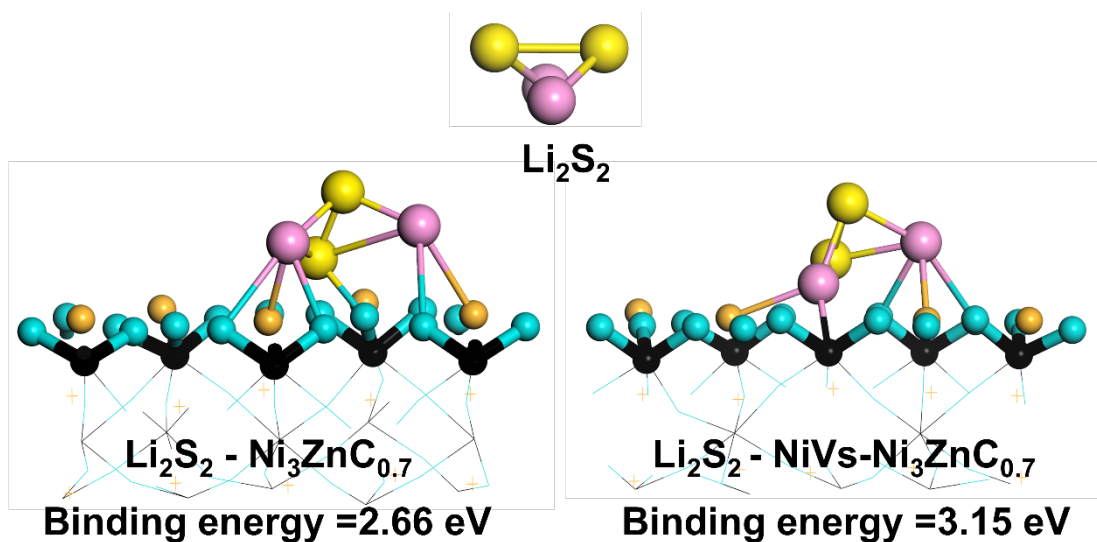


Fig. S4. DFT calculation optimized configurations of  $\text{Li}_2\text{S}_2$  absorbed on  $\text{Ni}_3\text{ZnC}_{0.7}$  (111) and  $\text{NiVs-Ni}_3\text{ZnC}_{0.7}$  (111) surface.

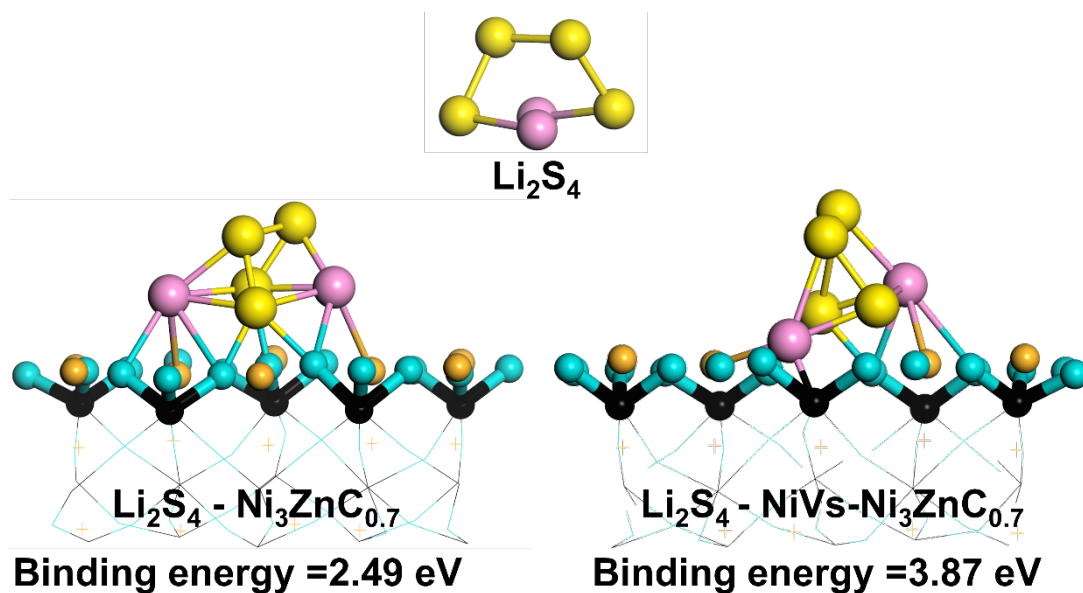


Fig. S5. DFT calculation optimized configurations of  $\text{Li}_2\text{S}_4$  absorbed on  $\text{Ni}_3\text{ZnC}_{0.7}$  (111) and  $\text{NiVs-Ni}_3\text{ZnC}_{0.7}$  (111) surface.

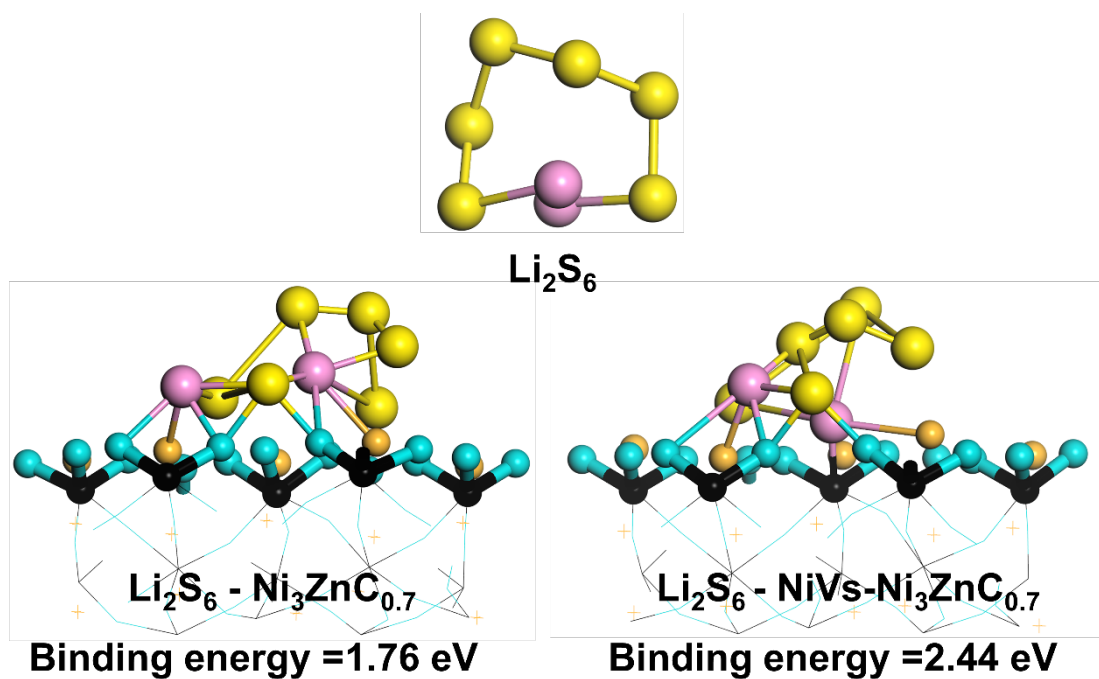


Fig. S6. DFT calculation optimized configurations of  $\text{Li}_2\text{S}_6$  absorbed on  $\text{Ni}_3\text{ZnC}_{0.7}$  (111) and  $\text{NiVs-Ni}_3\text{ZnC}_{0.7}$  (111) surface.

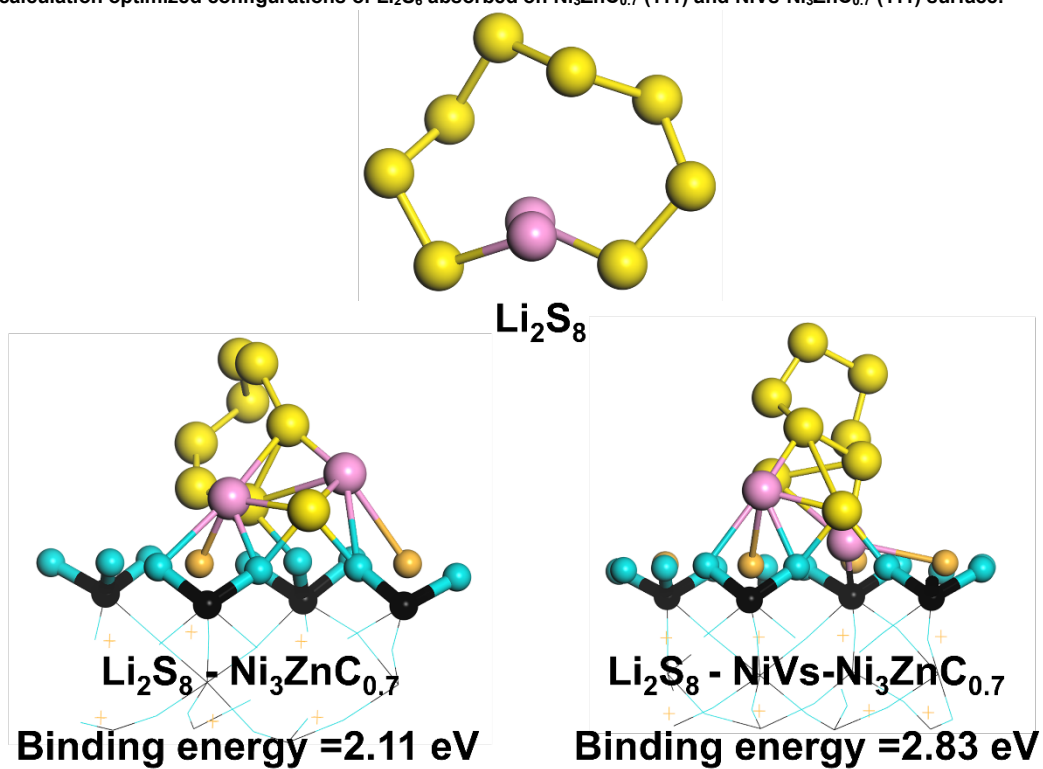


Fig.S7. DFT calculation optimized configurations of  $\text{Li}_2\text{S}_8$  absorbed on  $\text{Ni}_3\text{ZnC}_{0.7}$  (111) and  $\text{NiVs-Ni}_3\text{ZnC}_{0.7}$  (111) surface.

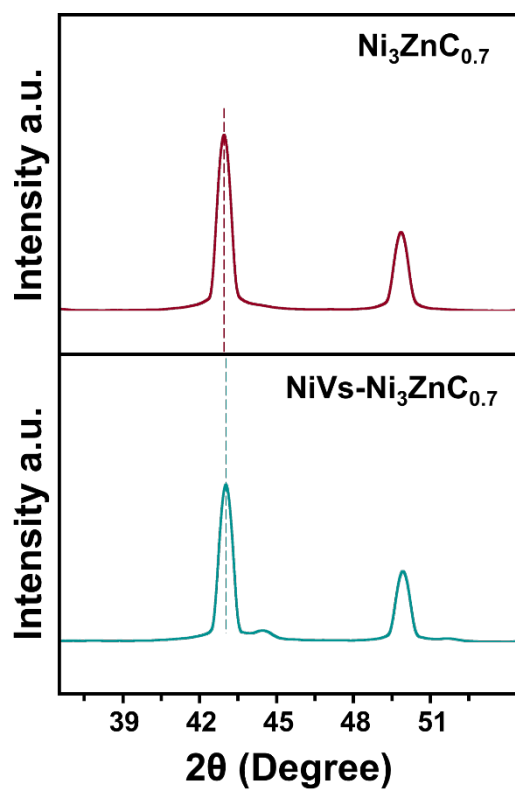


Fig. S8. XRD patterns of  $\text{Ni}_3\text{ZnC}_{0.7}$  and  $\text{NiVs-Ni}_3\text{ZnC}_{0.7}$ .

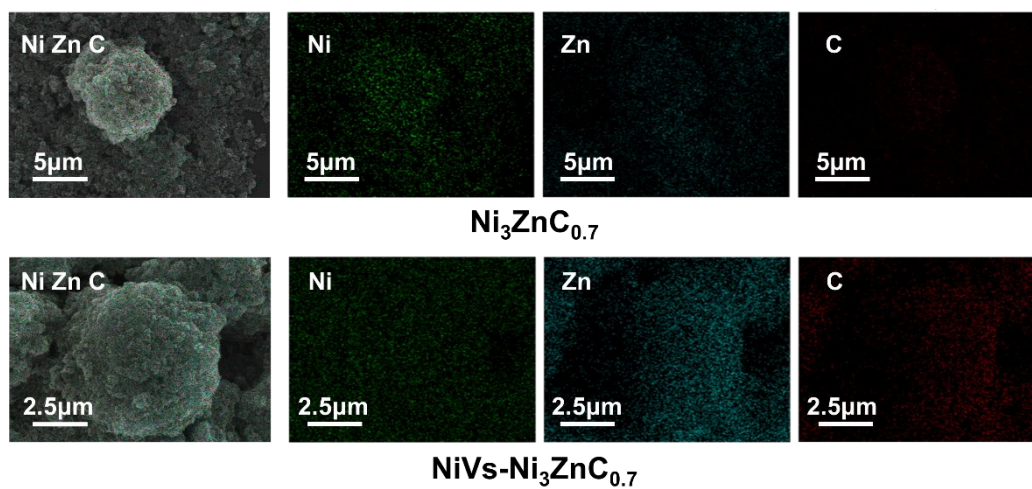


Fig. S9. SEM images of  $\text{Ni}_3\text{ZnC}_{0.7}$  and  $\text{NiVs-Ni}_3\text{ZnC}_{0.7}$  and the corresponding elemental mapping images.

**Table S1** Comparison of electrochemical performance of Li-S batteries with possible catalysts

Catalysts	Electrolyte recipes	Testing condition	Cyclability	Year	Ref.
PVs-CoP	1 M LiTFSI DME/DOL + 2.0 wt% LiNO <sub>3</sub>	2.0 C	585 mA h g <sup>-1</sup> after 300 cycles	2022	4
OVs-STMn <sub>0.3</sub>	1 M LiTFSI DME/DOL + 2.0 wt% LiNO <sub>3</sub>	2.0 C	406 mA h g <sup>-1</sup> after 1500 cycles	2022	5
NVs-TiN	1 M LiTFSI DME/DOL + 2.0 wt% LiNO <sub>3</sub>	2.0 C	576 mA h g <sup>-1</sup> after 600 cycles	2019	6
OVs-TiO <sub>2</sub>	1 M LiTFSI DME/DOL + 0.1 M LiNO <sub>3</sub>	2.0 C	631 mA h g <sup>-1</sup> after 500 cycles	2020	7
Single Ni @N-doped graphene	1 M LiTFSI DME/DOL + 1.0 wt% LiNO <sub>3</sub>	1.0 C	826 mAh g <sup>-1</sup> after 500 cycles	2019	8
NiVs-Ni <sub>3</sub> ZnC <sub>0.7</sub>	1 M LiTFSI DME/DOL + 2.0 wt% LiNO <sub>3</sub>	0.5C	686 mAh g <sup>-1</sup> after 1000 cycles	2022	This work

## References

1. P. E. Blochl, *Physical Review B*, 1994, **50**, 17953-17979.
2. J. P. Perdew, K. Burke and M. Ernzerhof, *Physical Review Letters*, 1996, **77**, 3865-3868.
3. Y. Wang, W. T. Wu, Y. Rao, Z. T. Li, N. Tsubaki and M. B. Wu, *J Mater Chem A*, 2017, **5**, 6170-6177.
4. R. Sun, Y. Bai, Z. Bai, L. Peng, M. Luo, M. X. Qu, Y. C. Gao, Z. H. Wang, W. Sun and K. N. Sun, *Adv Energy Mater*, 2022, **12**, 2102739.
5. W. S. Hou, P. L. Feng, X. Guo, Z. H. Wang, Z. Bai, Y. Bai, G. X. Wang and K. N. Sun, *Adv Mater*, 2022, **34**, 2202222.
6. Y. Yao, H. Y. Wang, H. Yang, S. F. Zeng, R. Xu, F. F. Liu, P. C. Shi, Y. Z. Feng, K. Wang, W. J. Yang, X. J. Wu, W. Luo and Y. Yu, *Adv Mater*, 2020, **32**, 1905658.
7. Z. Li, C. Zhou, J. Hua, X. Hong, C. Sun, H.-W. Li, X. Xu and L. Mai, *Adv Mater*, 2020, **32**, 1907444.
8. L. L. Zhang, D. B. Liu, Z. Muhammad, F. Wan, W. Xie, Y. J. Wang, L. Song, Z. Q. Niu and J. Chen, *Adv Mater*, 2019, **31**, 1900009.